

## Biosensing with a scanning planar Yagi-Uda antenna: supplement

**NAVID SOLTANI,<sup>1,2,\*</sup>  ELHAM RABBANY ESFAHANY,<sup>1,2</sup> SERGEY I. DRUZHININ,<sup>2,3</sup>  GREGOR SCHULTE,<sup>2,3</sup> JULIAN MÜLLER,<sup>2,4</sup> BENJAMIN BUTZ,<sup>2,4</sup>  HOLGER SCHÖNHERR,<sup>2,3</sup>  MARIO AGIO,<sup>1,2,5</sup>  AND NEMANJA MARKEŠEVIĆ<sup>1,6</sup>**

<sup>1</sup>Laboratory of Nano-Optics, University of Siegen, Siegen 57072, Germany

<sup>2</sup>Research Center of Micro- and Nanochemistry and (Bio)Technology (Cμ), Siegen 57076, Germany

<sup>3</sup>Physical Chemistry I, University of Siegen, Siegen 57076, Germany

<sup>4</sup>Micro- and Nanoanalytics Group, University of Siegen, Siegen 57076, Germany

<sup>5</sup>National Institute of Optics (INO), National Research Council (CNR), Florence 50125, Italy

<sup>6</sup>Currently with Nanoscience Center, University of Jyväskylä, Jyväskylä 40014, Finland

\* [navid.soltani@uni-siegen.de](mailto:navid.soltani@uni-siegen.de)

This supplement published with Optica Publishing Group on 3 January 2022 by The Authors under the terms of the [Creative Commons Attribution 4.0 License](https://creativecommons.org/licenses/by/4.0/) in the format provided by the authors and unedited. Further distribution of this work must maintain attribution to the author(s) and the published article's title, journal citation, and DOI.

Supplement DOI: <https://doi.org/10.6084/m9.figshare.17161109>

Parent Article DOI: <https://doi.org/10.1364/BOE.445402>

# Supplementary information for: biosensing with a scanning planar Yagi-Uda antenna

NAVID SOLTANI,<sup>1,2,\*</sup> ELHAM RABBANY ESFAHANY,<sup>1,2</sup> SERGEY I. DRUZHININ,<sup>2,3</sup> GREGOR SCHULTE,<sup>2,3</sup> JULIAN MÜLLER,<sup>2,4</sup> BENJAMIN BUTZ,<sup>2,4</sup> HOLGER SCHÖNHERR,<sup>2,3</sup> MARIO AGIO<sup>1,2,5</sup> AND NEMANJA MARKEŠEVIĆ<sup>1,6</sup>

<sup>1</sup>Laboratory of Nano-Optics, University of Siegen, Siegen 57072, Germany

<sup>2</sup>Research Center of Micro- and Nanochemistry and (Bio)Technology (Cμ), Siegen 57076, Germany

<sup>3</sup>Physical Chemistry I, University of Siegen, Siegen 57076, Germany

<sup>4</sup>Micro- and Nanoanalytics Group, University of Siegen, Siegen 57076, Germany

<sup>5</sup>National Institute of Optics (INO), National Research Council (CNR), Florence 50125, Italy

<sup>6</sup>Currently with Nanoscience Center, University of Jyväskylä, Jyväskylä 40014, Finland

\*navid.soltani@uni-siegen.de

## 1. Fluorescence background of the gold director

Figure S1a shows the surface roughness of a 10 nm gold film (Platypustech, AU.0100.CSS Square Coverslips) captured by an environmental scanning electron microscope (ESEM). The emission intensity and the spectra of the light collected from the gold-coated glass coverslip as a function of laser power are presented in Fig. S1b and c, respectively. The gold film autofluorescence originates from an electronic interband transition between the  $s - p$  conduction band and the  $d$  bands [1]. In thin films the surface roughness can cause additional resonances due to localized surface plasmon modes [2]. In our experiments, the gold director generates around 2-3 times higher background autofluorescence than the signal detected from the glass coverslip.

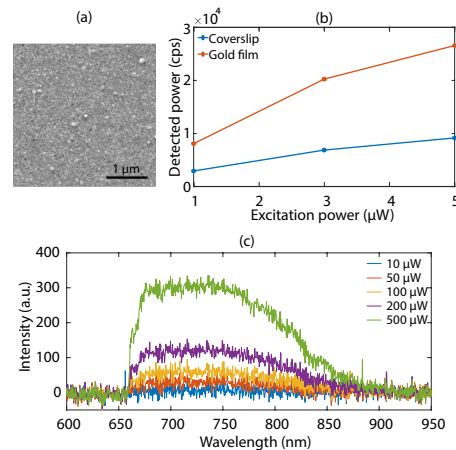


Fig. S1. **Characterization of the gold director.** (a) Environmental scanning electron microscope (ESEM) image of a 10 nm gold film (director) formed on a glass coverslip. (b) Detected power by a single-photon avalanche detector (SPAD) for low excitation powers (range used in the experiments). (c) Fluorescence spectrum of the gold director as a function of the excitation power using a long-pass filter (cutoff at 650 nm).

## 2. Bleaching time of ATTO-647N in T50 buffer

ATTO-647N (ATTO-TEC GmbH) dyes are subject to bleaching and, for a large ensemble of emitters, the intensity curve decays exponentially as presented in Fig. S2a (52 s for an ensemble of emitters). However, for samples with lower concentrations, the number of molecules in the focal area is small. In this case, bleaching and blinking of individual molecules significantly change the fluorescence signal and play an essential role in single-molecule detection. The results are shown for ATTO-647N labeled dsDNA molecules immobilized on coverslip [3,4] flow channels from buffered solutions with concentrations of 1 nM, 100 pM, and 10 pM in Fig. S2b-d, respectively. We use 2  $\mu$ W laser power in this set of measurements, except for samples prepared at a concentration of 100 pM (Fig. S2c), in which the excitation power is 6.6  $\mu$ W. In this way, we demonstrate that the emitters do not bleach immediately, even at higher excitation powers.

In Fig. S2b-d, the emission intensity changes in a step-wise manner as molecules blink and bleach randomly. The step sizes and the initial intensity can be used to estimate the number of molecules in the focal spot. Therefore, we conclude that at low concentrations, the bright spots typically contain less than ten emitters. Likewise, we expect a similar behaviour for ATTO-647N labeled dsDNA molecules immobilized on the gold director in the antenna configuration.

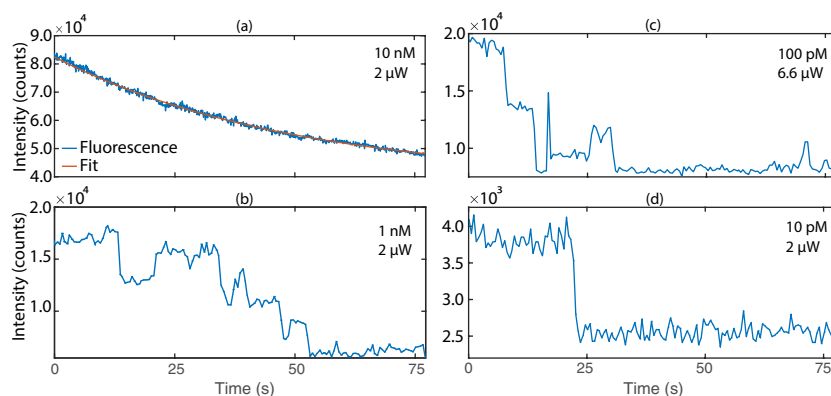


Fig. S2. **ATTO-647N bleaching and blinking in T50 buffer.** (a) Bleaching of ATTO-647N labeled dsDNA immobilized on a coverslip from a 10 nM solution. The experimental data fitted with a first-order exponential function (red curve) to find the bleaching time, which is approximately 52 s. (b-d) Step-wise bleaching and blinking of ATTO-647N labeled dsDNA from buffers with different concentrations immobilized on a coverslip: (b) 1 nM and 2  $\mu$ W excitation power, (c) 100 pM and 6.6  $\mu$ W excitation power, and (d) 10 pM and 2  $\mu$ W excitation power.

## 3. Signal deconvolution and decay rates fitting

As an example, the fluorescence decay of ATTO-647N molecules at the first maximum and minimum fluorescence intensity in Fig. 2b of the manuscript (circle and triangle positions) are shown in Fig. S3. The deconvolution process and fitting method is explained in the supporting information of Ref. [5]. At the circle position (Fig. S3a), due to higher signal counts, the decay fitting exhibits a lower error as compared to the triangle position (Fig. S3b).

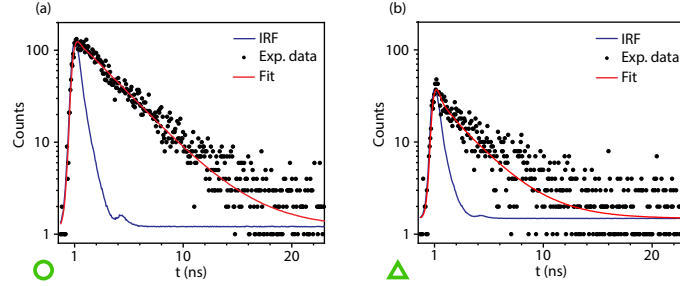


Fig. S3. **Fluorescence decay of ATTO-647N labeled dsDNA molecules in the planar antenna.** (a) Fluorescence decay at the first maximum of the fluorescence intensity shown in Fig. 2b (circle). SiO<sub>2</sub>-reflector distance 137 nm, decay rate  $\Gamma = 0.29 \text{ ns}^{-1}$ , fluorescence intensity  $P_{\text{flu0}} = 6767$  counts and background intensity (scattering of excitation light)  $P_{\text{bg}} = 1050$  counts. (b) Decay at the first minimum of the fluorescence intensity shown in Fig. 2b (triangle). SiO<sub>2</sub>-reflector distance 256 nm, decay rate  $\Gamma = 0.32 \text{ ns}^{-1}$ , fluorescence intensity  $P_{\text{flu0}} = 1277$  counts and background intensity  $P_{\text{bg}} = 394$  counts.

## References

1. A. Mooradian, "Photoluminescence of metals," Phys. Rev. Lett. **22**, 185 (1969).
2. H. Sun, M. Yu, G. Wang, X. Sun, and J. Lian, "Temperature-dependent morphology evolution and surface plasmon absorption of ultrathin gold island films," The J. Phys. Chem. C **116**, 9000–9008 (2012).
3. B. M. Reinhard, S. Sheikholeslami, A. Mastroianni, A. P. Alivisatos, and J. Liphardt, "Use of plasmon coupling to reveal the dynamics of DNA bending and cleavage by single EcoRV restriction enzymes," Proc. Natl. Acad. Sci. **104**, 2667–2672 (2007).
4. M. P. Busson, B. Rolly, B. Stout, N. Bonod, E. Larquet, A. Polman, and S. Bidault, "Optical and topological characterization of gold nanoparticle dimers linked by a single DNA double strand," Nano Lett. **11**, 5060–5065 (2011).
5. N. Soltani, E. Rabbany Esfahany, S. I Druzhinin, G. Schulte, J. Müller, B. Butz, H. Schönherr, N. Markešević, and M. Agio, "Scanning planar Yagi-Uda antenna for fluorescence detection," J. Opt. Soc. Am. B **38**, 2528–2535 (2021).